ISSN 1070-3284, Russian Journal of Coordination Chemistry, 2014, Vol. 40, No. 6, pp. 379–388. © Pleiades Publishing, Ltd., 2014.

Two Coordination Polymers from 2-*p*-Butylphenyl Imidazole Dicarboxylate: Syntheses, Crystal Structures, and Thermal Properties[1]

R. M. Gao, J. Li, M. W. Guo, and G. Li*

College of Chemistry and Molecular Engineering, Zhengzhou University, Zhengzhou, 450001 P.R. China

**e-mail: gangli@zzu.edu.cn*

Received June 5, 2013

Abstract—By employing a newly designed ligand, 2-(*p*-*tert*-butylphenyl)-1*H*-imidazole-4,5-dicarboxylic acid (H_3BuPhIDC) to react with manganese(II) or nickel(II) ions, two coordiantion polymers [$Mn_2(\mu_3$-HBuPhIDC)$_2(CH_3OH)_2$] (**I**) and [Ni(μ_2-HBuPhIDC)$(H_2O)_2$] (**II**) have been solvothermally synthesized and structurally characterized by elemental analyses, IR spectroscopy, and single crystal X-ray diffraction. Polymer **I** shows a 3D framework bearing 1D octagonal channels constructed from left- and right-handed helical chains. Polymer **II** exhibits an infinite chain structure, which are joined through the π–π interactions and intramolecular hydrogen bonds to form a 3D architecture. The thermal properties of the polymers have been investigated as well. The coordination ability and modes of H_3BuPhIDC have been investigated from both theoretical and experimental aspects.

DOI: 10.1134/S1070328414050042

INTRODUCTION

In recent years, design and construction of functional coordination polymers (CPs) via metal ions and various organic ligands have become a hot research area. Imidazole-4,5-dicarboxylates (H_3IDC) and its derivatives, which have six potential donor atoms: two imidazole nitrogen atoms and four carboxylate oxygen atoms, have attracted much attention due to their strong coordination ability and variety coordination modes [1–4].

More recently, our laboratory has synthesized a series of imidazole dicarboxylate ligands bearing 2-position phenyl-groups, for example, 2-phenyl-1*H*-imidazole-4,5-dicarboxylic acid (H_3PhIDC), 2-methylphenyl-1*H*-imidazole-4,5-dicarboxylic acid (H_3MePhIDC) and 2-dimethylphenyl-1*H*-imidazole-4,5-dicarboxylic acid (H_3DMPhIDC) [5–7], and successfully obtained some fascinating structures, such as 3D polymer [Mn(μ_3-HPhIDC)$(H_2O)_2$] composed of novel 2D stairlike layers in the *yz* plane, 3D interpenetrating framework {[$Co_{1.5}$(*p*-MePhIDC)$(H_2O)_3$] · H_2O}$_n$ containing honeycomb-like cages, and 3D polymer {[$Co_3(\mu_3$-DMPhIDC)$_2(H_2O)_6$] · $2H_2O$}$_n$ bearing infinite 1D hexagonal channels and [Co_2(DMPhIDC)]$_6$ cages. As one might expect, the relative orientations of the imidazole dicarboxylate is a key factor to determine the structures of the MOFs. Changes in the substituents on the phenyl ring to which the imidazole dicarboxylate units are attached may result in different spatial arrangements of the MOFs. At the same time, our findings indicated that the bulky aromatic group can supply additional stabilizing forces for solid-state crystallizing packing.

Encouraged by our preliminary studies, we continuously investigate butylphenyl substituted imidazole dicarboxylate ligand at 2-position and successfully prepare a new organic ligand, 2-(*p*-*tert*-butylphenyl)-1*H*-imidazole-4,5-dicarboxylic acid (H_3BuPhIDC), and hope to explore its coordination features. To our excitement, two MOFs, namely [$Mn_2(\mu_3$-HBuPhIDC)$_2(CH_3OH)_2$] (**I**) and [Ni(μ_2-HBuPhIDC)$(H_2O)_2$] (**II**), have been synthesized (Scheme). In this paper, we will present the crystal structures and thermal properties of the two coordination polymers **I** and **II**, and describe the coordination modes of $HBuPhIDC^{2-}$ anions (Fig. 1).

[1] The article is published in the original.

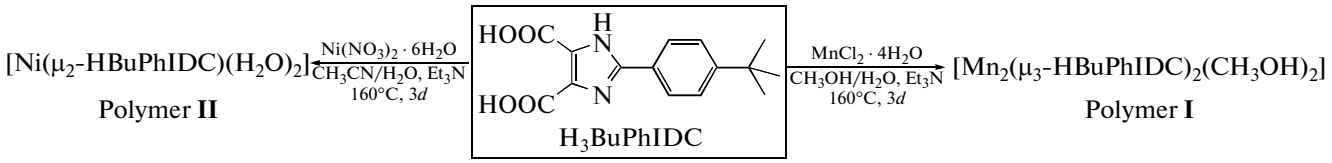

Scheme.

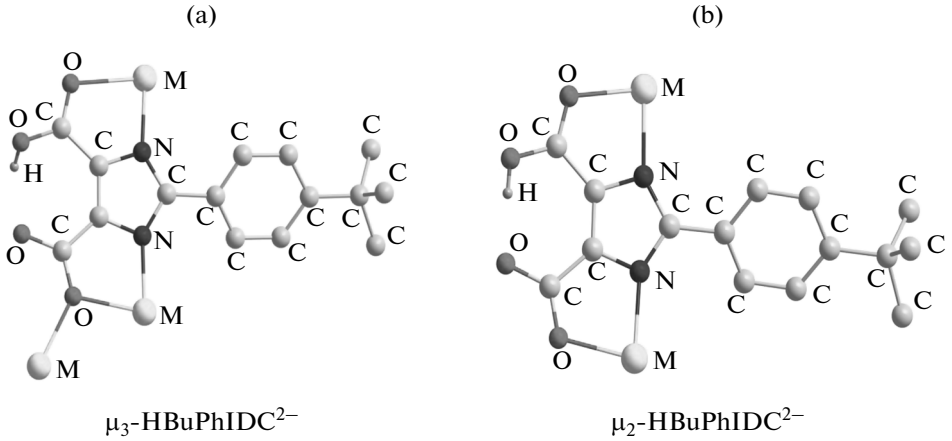

Fig. 1. Coordination modes of $HBuPhIDC^{2-}$ anions in polymers **I** (a) and **II** (b).

EXPERIMENTAL

All chemicals were of reagent grade quality obtained from commercial sources and used without further purification. The organic ligand $H_3BuPhIDC$ was prepared according to literature procedure [8]. The C, H, and N microanalyses were carried out on a FLASH EA 1112 analyzer. IR spectra were recorded on a BRUKER TENSOR 27 spectrophotometer as KBr pellets in the 400–4000 cm^{-1} region. TG measurements were performed by heating the crystalline sample from 20 to 680°C at a rate of 10°C min^{-1} in the air on a Netzsch STA 409PC differential thermal analyzer.

Synthesis of I. A mixture of $MnCl_2 \cdot 4H_2O$ (10.1 mg, 0.05 mmol), $H_3BuPhIDC$ (14.5 mg, 0.05 mmol) $CH_3OH–H_2O$ (3 : 4, 7 mL), Et_3N (0.014 mL, 0.1 mmol) were sealed in a 25 mL Teflon-lined stainless steel autoclave, heated at 160°C for three days, and then cooled to room temperature. Colorless lamellar crystals of **I** were isolated, washed with distilled water, and dried in air (39% yield based on Mn).

IR (KBr; ν, cm^{-1}): 3430 m, 2959 m, 1597 s, 1573 s, 1491 m, 1405 s, 1363 w, 1344 m, 1116 w, 841 w, 715 w.

For $C_{32}H_{34}N_4O_{10}Mn_2$

anal. calcd., %:	C, 51.57;	H, 4.56;	N, 7.52.
Found, %:	C, 51.79;	H, 4.28;	N, 7.34.

Synthesis of II. A mixture of $Ni(NO_3)_2 \cdot 6H_2O$ (14.5 mg, 0.05 mmol), $H_3BuPhIDC$ (14.5 mg, 0.05 mmol) $CH_3CN–H_2O$ (3 : 4, 7 mL), Et_3N (0.014 mL, 0.1 mmol) were sealed in a 25 mL Teflon-lined stainless steel autoclave, heated at 160°C for three days, and then cooled to room temperature. Glitter green block–shape crystals of **II** were isolated, washed with distilled water, and dried in air (51% yield based on Ni).

IR (KBr; ν, cm^{-1}): 3592 m, 2965 m, 1707 w, 1621 m, 1560 s, 1493 m, 1435 s, 1365 w, 1281 w, 1130 w, 844 w, 760 w.

For $C_{15}H_{18}N_2O_6Ni$

anal. calcd., %:	C, 47.36;	H, 4.74;	N, 7.37.
Found, %:	C, 47.19;	H, 4.31;	N, 7.58.

X-ray crystallography. Measurements of compounds **I** and **II** were made on a Bruker smart APEXII CCD diffractometer with a graphite-monochromated MoK_α radiation (λ = 0.71073 Å). Single crystals of **I** and **II** were selected and mounted on a glass fiber. All data were collected at room temperature using the ω–2θ scan technique and corrected for Lorenz-polarization effects. A correction for secondary extinction was applied. The two structures were solved by direct methods and expanded using the Fourier technique. The non-hydrogen atoms were refined with anisotropic thermal parameters. Hydrogen atoms were included but not refined. The final cycle of full-matrix least squares refinement was based on 7047 observed reflections and 443 variable parameters for **I**, 3739 observed reflections and 233 variable parameters for **II**. All calculations were performed using the SHELX-97 crystallographic software package [9]. Crystal data and experimental details for compounds **I** and **II** are contained in Table 1. Selected bond lengths and angles are listed in Table 2. Supplementary material has been deposited with the Cambridge Crystallographic Data Centre (nos. 895529 and 913637 for **I** and **II**, respectively; deposit@ccdc.cam.ac.uk or http://www.ccdc.cam.ac.uk).

Quantum-chemical calculation. The optimized geometry and natural bond orbital (NBO) charge distributions of the free ligand $H_3BuPhIDC$ were given by the GAUSSIAN 03 suite of programs [10].

Table 1. Crystal data and structure refinement information for compounds **I** and **II**

Parameter	Value	
	I	**II**
Temperature, K	296(2)	296(2)
Fw	744.51	381.02
Crystal system	Tetragonal	Orthorhombic
Crystal size, mm	0.23 × 0.20 × 0.19	0.22 × 0.20 × 0.20
Space group	$I\bar{4}$	*Ibca*
a, Å	20.6044(9)	12.0233(13)
b, Å	20.6044(9)	21.236(2)
c, Å	16.2760(14)	25.690(3)
V, Å^3	6909.8(7)	6559.3(12)
ρ_{calcd}, mg m^{-3}	1.431	1.543
Z	8	16
μ, mm^{-1}	0.791	1.217
Reflections Nillected/unique (R_{int})	19667/7047 (0.0708)	19075/3739 (0.0685)
Data/restraints/parameters	7047/0/443	3739/0/233
GOOF on F^2	0.950	1.032
R	0.0627	0.0390
wR	0.1585	0.1005
$\Delta\rho_{max}$ and $\Delta\rho_{min}$, *e* Å^{-3}	0.610 and –0.492	0.476 and –0.480

And all calculations were carried out at the B3LYP/6-311++G(d, p) level of theory.

RESULTS AND DISCUSSION

To obtain theoretical information for the ligand H_3BuPhIDC, we have investigated the *tert*-butyl-phenyl substituent effect in H_3BuPhIDC by theoretical calculation [10]. The computed results reveal that the free ligand H_3BuPhIDC has two characteristics: (1) The negative NBO charges mainly distribute on the oxygen and nitrogen atoms. The NBO charges are –0.636, –0.648, –0.666, and –0.599 for four carboxylate oxygen atoms, –0.460 and –0.498 for two imidazole nitrogen atoms (Fig. 2, Table 3). These values indicate that the oxygen and nitrogen atoms of the ligand all have potential coordination ability. So H_3BuPhIDC may show superior strong coordination ability under appropriate conditions. This finding can be confirmed by our present experimental results. (2) As shown in Table 3, compared with the free ligand PhH_3IDC [5], the introduction of 2-*tert*-butyl group into H_3BuPhIDC, has slight effect on the NBO charge distributions of oxygen and nitrogen atoms. That is to say, the substituent effect of 2-*tert*-butyl group is slight. Although it should be given more consideration on

Table 2. Selected bond distances (Å) and angles (deg) for the complexes **I** and **II***

Bond	*d*, Å	Bond	*d*, Å	Bond	*d*, Å
		I			
Mn(1)–N(1)	2.024(6)	Mn(1)–N(3)$^{\#1}$	2.074(6)	Mn(1)–O(9)	2.126(6)
Mn(1)–O(3)	2.173(5)	Mn(1)–O(6)	2.244(5)	Mn(1)–O(1)	2.297(6)
Mn(2)–N(2)	2.036(6)	Mn(2)–N(4)$^{\#2}$	2.071(6)	Mn(2)–O(7)	2.094(6)
Mn(2)–O(3)	2.178(5)	Mn(2)–O(6)	2.197(5)	Mn(2)–O(4)	2.280(5)
		II			
Ni(2)–N(2)	2.090(2)	Ni(1)–N(1)	2.122(2)	Ni(2)–O(1)	2.0526(18)
Ni(1)–O(4)	2.0795(19)	Ni(1)–O(5)	2.064(2)	Ni(2)–O(6)	2.106(2)
Angle	ω, deg	Angle	ω, deg	Angle	ω, deg
		I			
N(1)Mn(1)N(3)$^{\#1}$	117.2(2)	N(1)Mn(1)O(9)	112.0(2)	N(3)$^{\#1}$Mn(1)O(9)	95.1(2)
N(1)Mn(1)O(3)	152.3(2)	N(3)$^{\#1}$Mn(1)O(3)	80.1(2)	O(9)Mn(1)O(3)	85.9(2)
N(1)Mn(1)O(6)	89.8(2)	N(3)$^{\#1}$Mn(1)O(6)	151.9(2)	O(9)Mn(1)O(6)	80.6(2)
O(3)Mn(1)O(6)	71.87(18)	N(1)Mn(1)O(1)	78.6(2)	N(3)$^{\#1}$Mn(1)O(1)	96.0(2)
O(9)Mn(1)O(1)	158.8(2)	O(3)Mn(1)O(1)	78.21(19)	O(6)Mn(1)O(1)	81.1(2)
N(2)Mn(2)N(4)$^{\#2}$	111.5(2)	N(2)Mn(2)O(7)	109.8(2)	N(4)$^{\#2}$Mn(2)O(7)	100.3(2)
N(2)Mn(2)O(3)	95.0(2)	N(4)$^{\#2}$Mn(2)O(3)	150.8(2)	O(7)Mn(2)O(3)	81.1(2)
N(2)Mn(2)O(6)	157.7(2)	N(4)$^{\#2}$Mn(2)O(6)	78.2(2)	O(7)Mn(2)O(6)	87.1(2)
O(3)Mn(2)O(6)	72.69(18)	N(2)Mn(2)O(4)	79.6(2)	N(4)$^{\#2}$Mn(2)O(4)	92.8(2)
O(7)Mn(2)O(4)	159.3(2)	O(3)Mn(2)O(4)	79.7(2)	O(6)Mn(2)O(4)	79.89(19)
		II			
O(5)$^{\#1}$Ni(1)O(5)	79.18(12)	O(5)$^{\#1}$Ni(1)N(1)	100.76(9)	O(4)Ni(1)O(4)$^{\#1}$	92.84(11)
O(4)Ni(1)N(1)	81.23(8)	O(1)Ni(2)O(6)	91.39(8)	O(4)Ni(1)N(1)$^{\#1}$	88.11(8)
O(1)Ni(2)N(2)	97.48(8)	N(2)Ni(2)O(6)	87.75(8)	O(5)Ni(1)N(1)	91.18(9)
O(5)$^{\#1}$Ni(1)O(4)	172.92(8)	O(5)Ni(1)O(4)	94.02(8)	N(1)$^{\#1}$Ni(1)N(1)	164.54(13)

* Symmetry transformations used to generate equivalent atoms: $^{\#1}$ $x, -y+1, -z+2$; $^{\#2}$ $x-1/2, -y+1/2, z+3/2$ (**I**); $^{\#1}$ $x+1/2, y, -z$ (**II**).

bulky aromatic groups in the ligand, it can be predicted that the strong coordination ability can suppress the steric effect of the aromatic group.

A single-crystal X-ray diffraction study shows that compound **I** is the open 3D structure crystallizing in the tetragonal space group $I\bar{4}$. The asymmetrical unit of **I** consists of two Mn^{2+} cations, two discrete $HBuPhIDC^{2-}$ ligands, as well as two coordination methanol molecules. Two Mn atoms in the center position here are associated with a center inversion operation. Each of them is in a slightly distorted octahedral geometry [MnN_2O_4]: two imidazole nitrogen (N(2) and N(4b)) and two carboxylate oxygen atoms (O(4) and O(6)) from two individual $HBuPhIDC^{2-}$ anions, one carboxylate oxygen atom (O(3)) from another one μ-bridging $HBuPhIDC^{2-}$ anion, and one oxygen atom

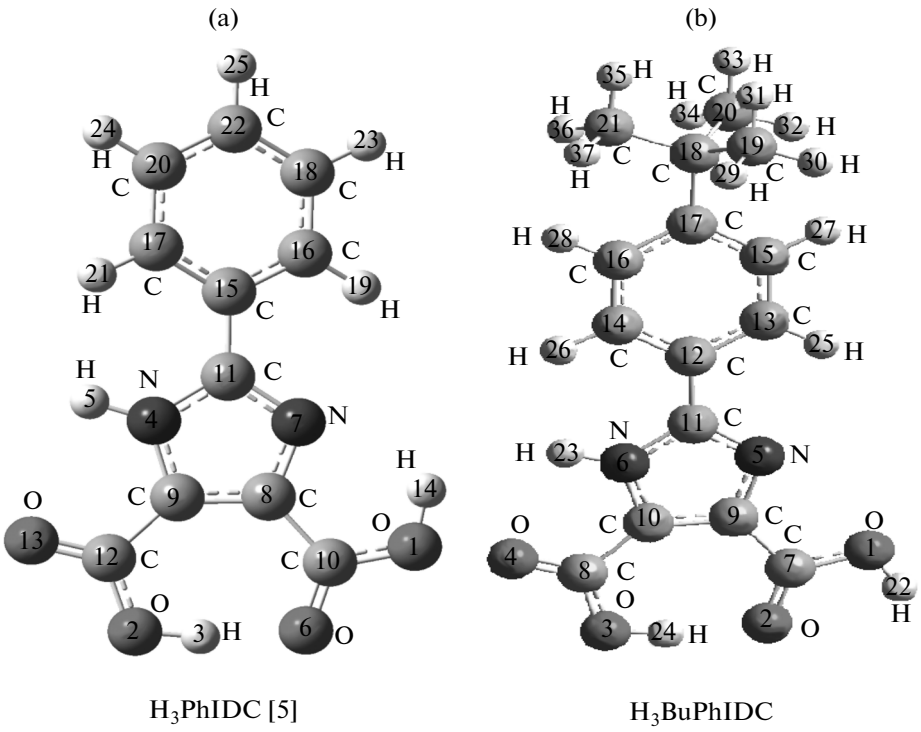

Fig. 2. Optimized geometries of the free ligands H_3PhIDC [5] (a) and H_3BuPhIDC (b).

(O7) from the coordinated methanol molecule (Fig. 3a). The Mn–N bond lengths are in the range of 2.024(6)–2.074(6) Å, while the Mn–O distances span from 2.094(6) to 2.297(6) Å. The bond angles around the central Mn^{2+} ion vary from 71.87(18)° to 158.8(12)°. The bond lengths and angles within the $HBuPhIDC^{2-}$ ligand have no significant difference from those reported in the literature [7].

The ligand $HBuPhIDC^{2-}$ in complex **I** adopts the coordination mode linking three Mn atoms by μ_3-*k*N, O: *k*O: *k*N', O' mode (Fig. 1a). The distance between the two dinuclear Mn^{2+} ions is 3.5493(12) Å. As viewed from the *xz* plane (Fig. 1b), neighboring Mn atoms are also linked by $HBuPhIDC^{2-}$ anions to form 1D left-handed and 1D right-handed helix chains, and are further bridged by O atoms of the carboxylate groups to form a diamond-shaped 2D layer. These helical chains are built by the $N_{imidazole}$ of $HBuPhIDC^{2-}$ ligands bridging neighboring metal centers. Interestingly, the individual ring structures as the secondary building units present clearly in the grid, while the ring structure looks as a rhombus window of approximate dimensions 10.4244 × 10.4244 Å.

It should be pointed out that eight Mn^{2+} ions are linked by twelve $HBuPhIDC^{2-}$ ligands to form one $[Mn_2(HBuPhIDC)_3]_4$ cage (Fig. 3c). Furthermore, these cages are shared with Mn(II) atoms to yield a 3D framework with 1D channels (Fig. 3d). In order to get better understanding of the 3D network, we simplified this through topological considerations (Fig. 3e).

To the best of our knowledge, Mn(II) coordination polymers with the imidazole dicarboxylate ligands were only found in recent publications [5–7, 11–17]. Only five 3D coordination polymers have been reported. Among them, polymers $[Mn_{1.5}(\mu_3\text{-PhIDC})(H_2O)_3]$ and $[Mn(\mu_3\text{-PhHIDC})(H_2O)]_2\}$ [5] were constructed by H_3PhIDC ligand. Polymer $\{[Mn_3(\mu_3\text{-DMPhIDC})_2(H_2O)_6] \cdot 2H_2O\}_n$ [11] were built by H_3DMPhIDC ligand. Polymers $\{[Mn(HPIDC)(H_2O)] \cdot 2H_2O\}_n$ [14] and $[Mn_3(Tmidc)_2(H_2O)_4] \cdot (H_2O)_6$ [15] were hydrothermally synthesized with the ligands of the H_3PIDC and the H_3Tmidc, respectively. In this paper, **I** has charming structure and is the second example of Mn(II) coordination polymer bearing $[Mn_2(HBuPhIDC)_3]_4$ cages.

Compound **II** crystallizes in the orthorhombic space group *Ibca*. The asymmetry unit of **II** contains one Ni^{2+} ion, one $HBuPhIDC^{2-}$ ligand with O, N chelating donors, and two terminal water molecules. What's more, the two Ni^{2+} ions assume similar distorted octahedral environments (Fig. 4a), in which four oxygen atoms of two $HBuPhIDC^{2-}$ ligands and two co-

Table 3. Natural bond orbital charge distributions of the free ligands H_3BuPhIDC and H_3PhIDC

Atom number	NBO charge	Atom number	NBO harge
H_3PhIDC [5]			
O(1)	–0.66493	C(17)	–0.19503
O(6)	–0.65884	C(18)	–0.20781
O(2)	–0.69007	C(20)	–0.20658
O(13)	–0.64991	C(22)	–0.19635
N(7)	–0.51400	H(3)	0.50658
N(4)	–0.49039	H(5)	0.48002
C(10)	0.80755	H(14)	0.54077
C(8)	0.02176	H(19)	0.23323
C(9)	0.06282	H(21)	0.22633
C(12)	0.77880	H(23)	0.22685
C(11)	0.40655	H(24)	0.22757
C(15)	–0.08825	H(25)	0.22604
C(16)	–0.18271		
H_3BuPhIDC			
O(1)	–0.636	C(20)	–0.560
O(2)	–0.648	C(21)	–0.576
O(3)	–0.666	H(22)	0.487
O(4)	–0.599	H(23)	0.437
N(5)	–0.460	H(24)	0.504
N(6)	–0.498	H(25)	0.232
C(7)	0.790	H(26)	0.194
C(8)	0.761	H(27)	0.206
C(9)	0.027	H(28)	0.212
C(10)	0.057	H(29)	0.205
C(11)	0.395	H(30)	0.200
C(12)	–0.112	H(31)	0.201
C(13)	–0.142	H(32)	0.200
C(14)	–0.160	H(33)	0.201
C(15)	–0.202	H(34)	0.205
C(16)	–0.211	H(35)	0.207
C(17)	0.006	H(36)	0.203
C(18)	–0.101	H(37)	0.203
C(19)	–0.560		

ordination water molecules are located in the equatorial position and two symmetry-related nitrogen atoms of two $HBuPhIDC^{2-}$ ligands are in the apical position. The Ni–O and Ni–N bond lengths are in the range of 2.0526(1)–2.106(2) Å and 2.090(2)–2.122(2) Å, respectively, which are consistent with those of previous reported compounds [18, 19]. In addition, the distance between the neighbouring two Ni^{2+} ions is 6.469 Å.

It is remarkable that the Ni atoms are joined by doubly deprotonated μ_2-$HBuPhIDC^{2-}$ ligands with the mode of μ_2-*k*N,O: *k*N',O' (Fig. 1b) to generate an infinite chain along the *z* axis (Fig. 4b) and each μ_2-$HBuPhIDC^{2-}$ ligand provides both chelating ligand and bridging ligand. Notably, a 2D metal-organic framework is constructed by the π–π interactions (the distance and dihedral between the two staggered phenyl rings is 6.5011 Å and 0°) and the intramolecular hydrogen bonds (O(5)–H(5)···O(3c), O(2)–H(2)···O(3) and O(6)–H(3)···O(2d)) between the chains along the *yz* axes and the layers pack each other through van der Waals interactions forming a 3D supramolecular architecture (Fig. 4c).

As far as we know, Ni(II) coordination polymers with imidazole dicarboxylate ligands are limited. Only one 2D polymer $[Ni(HPyIDC)(H_2O)]_n$ [18], one 1D polymer $[Ni(\mu_2\text{-}HMOPhIDC)(2,2'\text{-}Bipy)]_n$ [19], and one molecular square tetranuclear Ni(II) complex $[Ni_4(HEIDC)_4(H_2O)_8] \cdot 2H_2O$ [13] have recently been reported. The compound **II** is the first example of complex with the ligand 2-(*p-tert*-butylphenyl)-1*H*-imidazole-4,5-dicarboxylic acid. The successful preparation of polymer **II** gives us more chance to study its properties.

Compounds **I** and **II** indicate strong and broad absorption bands in the range of 3400–3500 cm^{-1}, which indicate the presence of the ν(N–H) and the ν(O–H) stretching frequencies of imidazole ring and water molecules. They exhibit strong characteristic absorptions around 1540–1660 cm^{-1} $\nu_{as}(COO^-)$ and 1400–1475 cm^{-1} $\nu_s(COO^-)$. The frame vibration of phenyl ring is observed at 1405 and 1435 cm^{-1} for **I** and **II**, respectively. The characteristic IR band of the tertbutyl at 1360–1380 cm^{-1} due to δ(=C–H) vibrations, which can be found at 1363 and 1365 cm^{-1} for **I** and **II**, respectively.

In order to estimate the thermal stabilities of the polymers, thermal gravimetric analyses (TGA) of **I** and **II** were carried out in the air (Fig. 5).

TG curve of polymer **I** suggests that it has good thermal stability before 354.3°C. When the temperature is higher than 354.3°C, the 3D framework starts decomposing. The weight loss of 78.35% in the range of 354.3–439.6°C corresponds to the decomposition

(a)

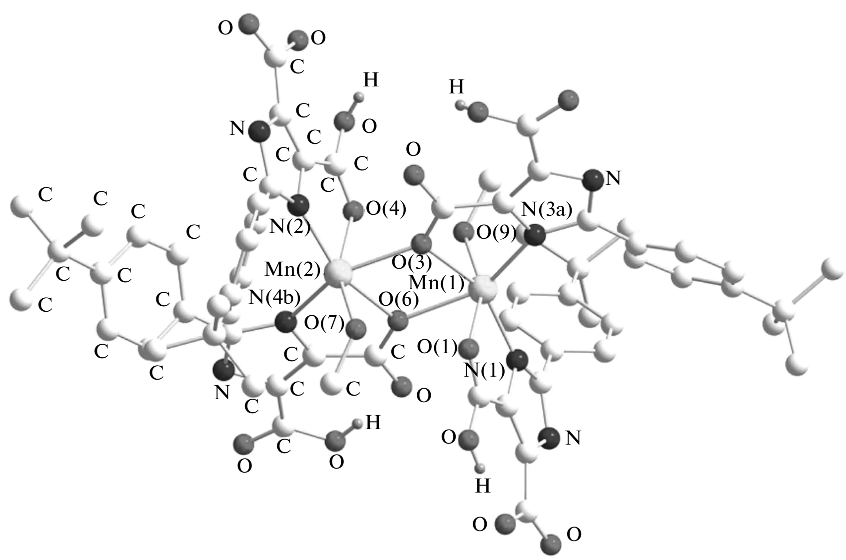

(b)

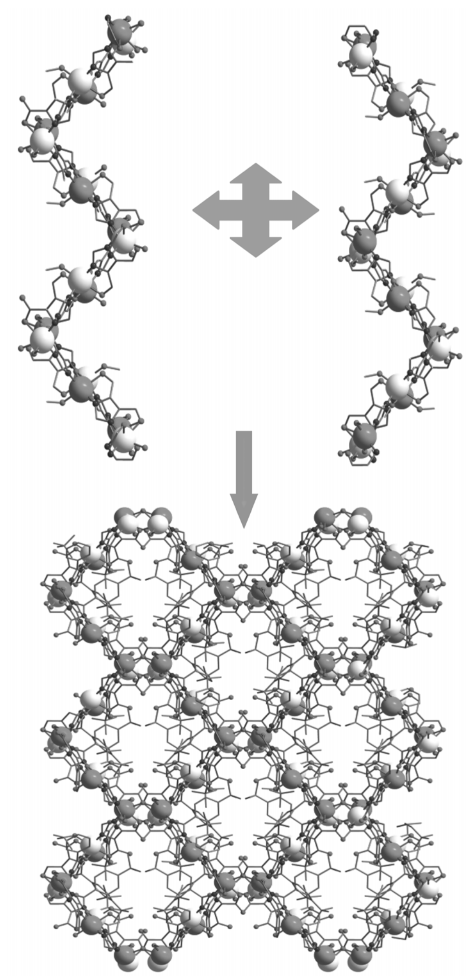

Fig. 3. Coordination environments of the Mn(II) atoms in **I** (a); the layer of complex **I** viewed along the *y* axis (in order to label the left- and right-handed helical chains we magnify the two lines of Mn(II) atoms in the middle) (b); view of the $[Mn_2(HBuPhIDC)_3]_4$ cage (c); view of the 3D framework of **I** with 1D channels (with partly atoms omitted for clarity) (d); the simplified topological consideration of the 3D network of **I** (e).

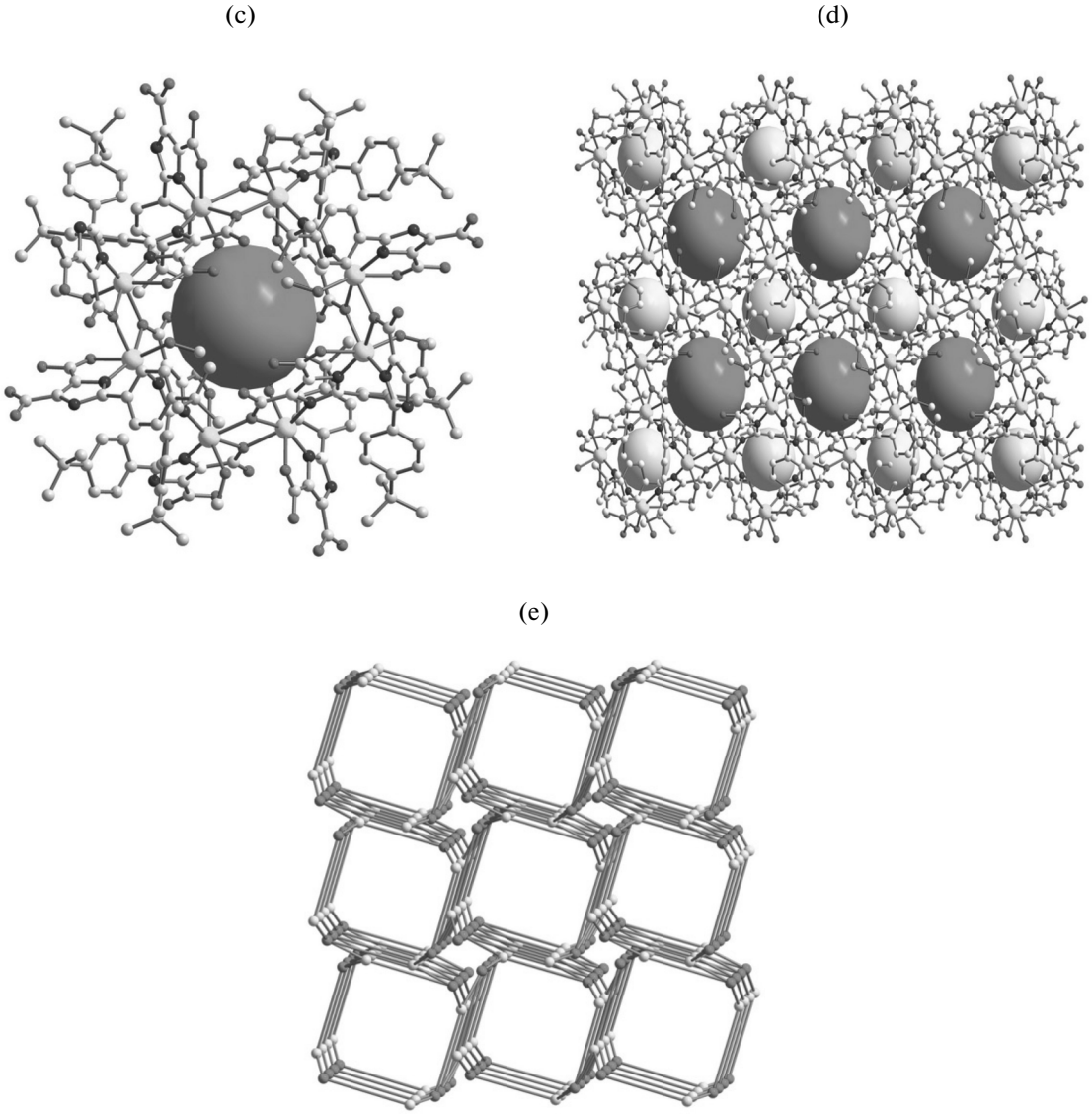

Fig. 3. (Contd).

of the $HBuPhIDC^{2-}$ group (calculated 80.91%). Subsequently, a plateau region is observed from 439.6 to 700.3°C. A white amorphous residue is 2MnO (observed 21.65%, calculated 21.83%).

The TG curve of polymer **II** reveals that the first weight loss from 119.2 to 281.6°C corresponds to the removal of the two coordination water molecules (observed 10.47%, calculated 9.47%). It keeps losing weight from 281.6 to 490.0°C, which may be ascribed to the decomposition of the organic $HBuPhIDC^{2-}$ ligand (observed 71.06%, calculated 71.05%). Finally, a plateau region is observed from 490.0 to 689.6°C. The remaining weight residue is NiO (observed 18.47%, calculated 19.47%).

In summary, two transition-metal-organic architectures have been successfully prepared by using the newly designed ligand $H_3BuPhIDC$. Their molecular structures have been characterized by single-crystal X-ray diffraction, elemental analyses, thermal analyses, and IR spectra. Both the experimental results and theoretical calculation show that the coordination ability of the ligand $H_3BuPhIDC$ is strong and the coordination modes are flexible.

ACKNOWLEDGMENTS

We gratefully acknowledge the financial support by the National Natural Science Foundation of China (nos. 21071127 and J1210060), and Program for New

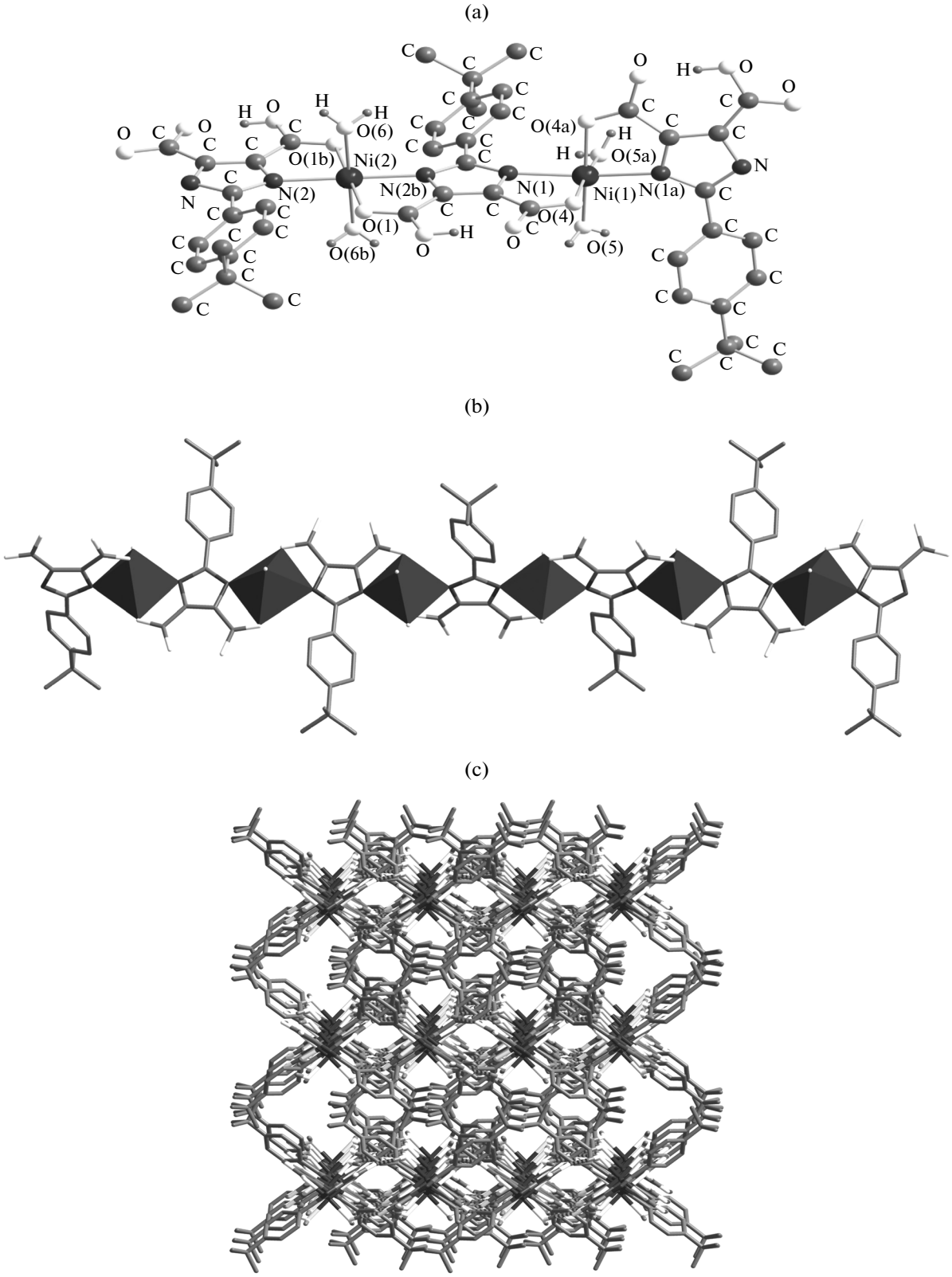

Fig. 4. Coordination environments of the Ni(II) atoms with atomic labels in **II** (a); view of the infinite chain structure of **II** (b); crystal packing diagram of **II** along the *z* axis showing the π–π stacking between the chains, containing intramolecular hydrogen bonds (c).

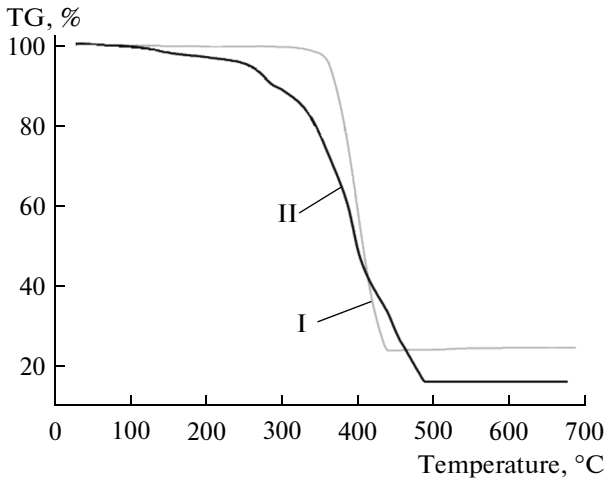

Fig. 5. TG analysis profiles of polymers **I** and **II**.

Century Excellent Talents in University (NCET-10-0139) and the Natural Science Foundation of Henan Education Department (nos. 2009A150028 and 2011A150029).

REFERENCES

1. Feng, X., Zhou, L.L., Wang, L.Y., et al., *Inorg. Chim. Acta*, 2013, vol. 394, p. 696.
2. Zhai, Q.G., Zeng, R.R., Li, S.N., et al., *CrystEngComm*, 2013, vol. 15, p. 965.
3. Li, Z.F., Luo, X.B., Gao, Y.C., et al., *Inorg. Chim. Acta*, 2012, vol. 384, p. 352.
4. Xiong, Z.F., Gao, R.M., Xie, Z.K., et al., *Dalton Trans.*, 2013, vol. 42, p. 4613.
5. Wang, W.Y., Yang, Z.L., Wang, C.J., et al., *CrystEngComm*, 2011, vol. 13, p. 4895.
6. Zhang, Y., Luo, X.B., Yang, Z.L., and Li, G., *CrystEngComm*, 2012, vol. 14, p. 7382.
7. Wang, C.J., Wang, T., Zhang, W., et al., *Cryst. Growth Des.*, 2012, vol. 12, p. 1091.
8. Lebedev, A.V., Lebedeva, A.B., Sheludyakov, V.D., et al., *Russ. J. Gen. Chem.*, 2007, vol. 77, p. 855.
9. Sheldrick, G.M., *SHELX-97*, Göttingen (Germany): Univ. of Göttingen, 1997.
10. Frisch, M.J., Trucks, G.W., Schlegel, H.B., et al., *GAUSSIAN 03, Revision C. 02*, Wallingford (CT, USA): Gaussian, Inc., 2004.
11. Wang, C.J., Wang, T., Li, L., et al., *Dalton Trans.*, 2013, vol. 42, p. 1715.
12. Zhang, F.W., Li, Z.F., Ge, T.Z., et al., *Inorg. Chem.*, 2010, vol. 49, p. 3776.
13. Song, J.F., Zhou, R.S., Hu, T.P., et al., *J. Coord. Chem.*, 2010, vol. 63, p. 4201.
14. Chen, L.Z., Huang, Y., Xiong, R.G., and Hu, H.W., *J. Mol. Struct.*, 2010, vol. 963, p. 16.
15. Xie, L.X., Hou, X.W., Fan, Y.T., and Hou, H.W., *Cryst. Growth Des.*, 2012, vol. 12, p. 1282.
16. Cao, X.J., Yang, Z.L., Guo, M.W., et al., *Synth. React. Inorg. Met.-Org. Chem.*, 2012, vol. 42, p. 402.
17. Lu, W.G., Gu, J.Z., Jiang, L., et al., *Cryst. Growth Des.*, 2008, vol. 8, p. 192.
18. Jing, X.M., Gong, S.Z., and Xiao, L.W., *Acta Crystallogr., E*, 2012, vol. 68, p. m187.
19. Cao, X.J., Liu, Y., Wang, L.Y., and Li, G., *Inorg. Chim. Acta*, 2012, vol. 392, p. 16.